Detecting the limit cycles for a class of Hamiltonian systems under thirteen-order perturbed terms

Gheorghe Tigan *

Abstract

It this paper we study a class of perturbed Hamiltonian systems under perturbations of thirteen order in order to detect the number of limit cycles which bifurcate from some periodic orbits of the unperturbed Hamiltonian system. The system has been previously studied in [9], [10], [11]. We observe in the present work that the system under perturbations of thirteen order can have more limit cycles than under perturbations of five [10], respectively nine [11] order but we have not identified more limit cycles than under perturbations of seven [9] order.

1 Introduction

Consider the following perturbed Hamiltonian system:

$$\begin{cases} \dot{x} = 4y\left(abx^2 - by^2 + 1\right) + \varepsilon x(ux^n + vy^n - b\frac{\beta+1}{\mu+1}x^\mu y^\beta - ux^2 - \lambda), \\ \dot{y} = 4x\left(ax^2 - aby^2 - 1\right) + \varepsilon y(ux^n + vy^n + bx^\mu y^\beta - vy^2 - \lambda) \end{cases} \tag{1}$$

where $\mu + \beta = n, 0 < a < b < 1, 0 < \varepsilon \ll 1$, u, v, λ are the real parameters and $n = 2k, k$ an integer positive. Studying the existence, number and distribution of limit cycles in a system of polynomial differential equations is an open problem even for a 2-degree polynomial and it is known as the Hilbert's 16th problem.

The system of differential equations:

$$\begin{cases} \dot{x} = y\left(1 + x^2 - ay^2\right) + \varepsilon x(mx^2 + ny^2 - \lambda) \\ \dot{y} = -x\left(1 - cx^2 + y^2\right) + \varepsilon y(mx^2 + ny^2 - \lambda) \end{cases} \tag{2}$$

has been discussed in [1], [8] and the system

$$\begin{cases} \dot{x} = y\left(1 - cy^2\right) + \varepsilon x(mx^2 + ny^2 - \lambda) \\ \dot{y} = -x\left(1 - ax^2\right) + \varepsilon y(mx^2 + ny^2 - \lambda) \end{cases} \tag{3}$$

in [7]. It has been shown that each of the two systems can have at least 11 limit cycles.

The higher order perturbations of the system (2), have been recently studied in [2], [3].

The following result is reported in [2].

---

*Department of Mathematics, "Politehnica" University of Timisoara, Timisoara, Timis, Romania; email: gtigan73@yahoo.com

THEOREM 1.1 *Consider the perturbed Hamiltonian system*

$$\dot{x} = -\frac{\partial H}{\partial y} + P(x, y, \alpha), \dot{y} = \frac{\partial H}{\partial x} + Q(x, y, \alpha) \tag{4}$$

Assume that $P(x, y, 0) = Q(x, y, 0) = 0$, and the unperturbed system exhibits a center. Denote by Γ^h the closed curves $H(x, y) = h$ surrounding this center, and by $\Gamma^h(D)$ the subset bounded by Γ^h and containing the center. Suppose that as h increases the diameter of the set $\Gamma^h(D)$ increases. If there exists h_0 such that function

$$A(h) = \int_{\Gamma^h(D)} [P''_{x\alpha}(x, y, 0) + Q''_{y\alpha}(x, y, 0)] dx dy \tag{5}$$

satisfies $A(h_0) = 0, A'(h_0) \neq 0, \alpha A'(h_0) < 0, respectively > 0$, then the perturbed system (4) has only one stable, respectively unstable limit cycle nearby Γ^{h_0}, for α very small. If Γ^h shrinks as h increases, the stability of the limit cycle is opposite to the above cases. If $A(h) \neq 0$, then the system (4) has no limit cycle.

The integral $A(h)$ is called the *Abelian integral* [16]. If the Hamiltonian system (4) is perturbed in the form:

$$\begin{cases} \dot{x}(t) = -\frac{\partial H}{\partial y} + \varepsilon x(p(x, y) - \lambda), \\ \dot{y}(t) = \frac{\partial H}{\partial x} + \varepsilon y(q(x, y) - \lambda), \end{cases} \tag{6}$$

where $p(0, 0) = q(0, 0) = 0$, then, by the above Theorem 1.1, from $A(h) = 0$, we get:

$$\lambda = \lambda(h) = \frac{\int_{\Gamma^h(D)} f(x, y) dx dy}{2 \int_{\Gamma^h(D)} dx dy}, \tag{7}$$

with $f(x, y) = x p'_x + y p'_y + p + q$. This function $\lambda(h)$ is called *the detection function* of the system (6).

Using the detection function $\lambda(h)$ we get by Theorem 1.1 the following result :

PROPOSITION 1.1 *a) If $(h_0, \lambda(h_0))$ is an intersecting point of a line $\lambda = \lambda_0$ and the detection curve $\lambda = \lambda(h)$, with $\lambda'(h_0) > 0 (< 0)$, then the system (6) has only one stable (unstable) limit cycle nearby Γ^{h_0}; b) If the line $\lambda = \lambda_0$ and the detection curve $\lambda = \lambda(h)$ do not intersect each other, then the system (6) has no limit cycle. If the $\Gamma^h(D)$ shrinks as h increases, the stability of the limit cycle is opposite to the above cases.*

This paper is organized as follows. In Section 2, we recall the results regarding the unperturbed system. In Section 3, using the analytical expressions of the detection functions and a Computer Algebra System we numerically compute the detection functions. Based on these data we can illustrate the distribution of the limit cycles.

2   The behavior of the unperturbed system

The unperturbed system (8) of the system (1) is:

$$\begin{cases} \dot{x} = 4y\left(-by^2 + abx^2 + 1\right) \\ \dot{y} = 4x\left(ax^2 - aby^2 - 1\right) \end{cases} \tag{8}$$

The Hamilton function defining this system is:

$$H(x,y) = -\left(ax^4 + by^4\right) + 2abx^2y^2 + 2\left(x^2 + y^2\right) = h \tag{9}$$

The function H has nine finite singular points:

$O(0,0), A_1\left(\sqrt{\frac{1+a}{a(1-ba)}}, \frac{1}{b-b^2a}\sqrt{b\left(1-ba\right)\left(1+b\right)}\right), A_2\left(\sqrt{\frac{1+a}{a(1-ba)}}, \frac{-1}{b-b^2a}\sqrt{b\left(1-ba\right)\left(1+b\right)}\right),$

$A_3\left(-\sqrt{\frac{1+a}{a(1-ba)}}, \frac{1}{b-b^2a}\sqrt{b\left(1-ba\right)\left(1+b\right)}\right), A_4\left(-\sqrt{\frac{1+a}{a(1-ba)}}, \frac{-1}{b-b^2a}\sqrt{b\left(1-ba\right)\left(1+b\right)}\right),$

$B_1(0,\sqrt{\frac{1}{b}}), B_2(0,-\sqrt{\frac{1}{b}}), C_1(\sqrt{\frac{1}{a}},0)$ and $C_2(-\sqrt{\frac{1}{a}},0)$.

Computing the eigenvalues of the associated linear system at each singular point we get that the points O, A_1, A_2, A_3, A_4 are centers, while B_1, B_2, C_1, C_2 are saddle points.

The values of the Hamilton function H at the singular points are respectively: $H(A_i) = \frac{2ba+b+a}{ba(1-ba)}, i = 1-4, H(B_k) = \frac{1}{b}, H(C_k) = \frac{1}{a}, k = 1,2$. Because $0 < a < b < 1$ we get that: $H(O) < H(B_1) < H(C_1) < H(A_1)$.

In polar coordinates, $x = r\cos\theta, y = r\sin\theta$, the system (8) becomes:

$$\dot{r} = -r^3 p'(\theta), \quad \dot{\theta} = -1 + r^2 p(\theta) \tag{10}$$

and the Hamilton function (9) gets:

$$H(r,\theta) = -r^4 p(\theta) + 2r^2 = h, \tag{11}$$

where

$$p(\theta) = a\cos^4\theta + b\sin^4\theta - 2ab\cos^2\theta\sin^2\theta. \tag{12}$$

REMARK 1 *The equilibrium points A_1, A_2, A_3, A_4 lie on the lines $d_\pm : \theta = \pm\arccos\sqrt{\frac{b+ba}{a+b+2ab}}$*

THEOREM 2.1 *As h varies on the real line, the level curves $H(x,y) = h$ can be classified, as follows [9]:*

1. $\Gamma_1^h : -\infty < h < 0$, *which corresponds to an orbit that surrounds all critical points (Fig.1a).*

2. $\Gamma_2^h \cup \Gamma_1^h : 0 \le h < \frac{1}{b}$, *corresponding to an orbit $\left(\Gamma_2^h\right)$ that surrounds only the point O and a curve of type $\left(\Gamma_1^h\right)$, (Fig.1b,a).*

3. $\Gamma_3^h : \frac{1}{b} < h < \frac{1}{a}$, *which corresponds to two symmetric orbits that do not cross the Oy axis, but encircle the rest of the critical points. If $h = \frac{1}{b}$ we get four heteroclinic orbits connecting the critical points B_1 and B_2 (Fig.2b,a).*

4. $\Gamma_4^h : \frac{1}{a} < h < \frac{2ba+b+a}{ba(1-ba)}$, *corresponding to four orbits that surround respectively the points $A_i, i = 1-4$. If $h = \frac{1}{a}$ we have four homoclinic orbits, namely, two homoclinic to C_1 and two homoclinic to C_2 (Fig.3b,a). Note that as h increases, the curves Γ_1^h, Γ_3^h and Γ_4^h shrink, while Γ_2^h extends.*
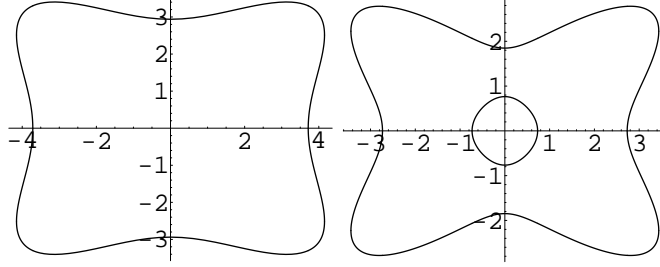
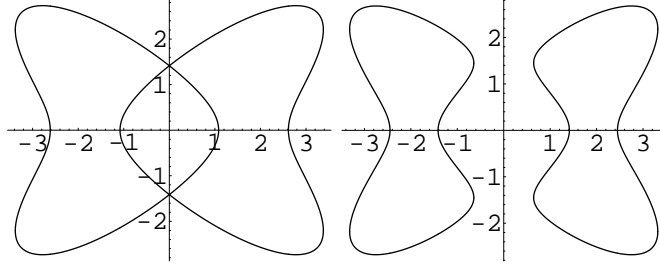Figure 1: Orbit of type a) L_1 (left) b) L_2 and L_1 (right)

Figure 2: a) Four heteroclinic orbits connecting two critical points B_1, B_2 (left) b) Two orbits of type L_3 (right)

3   Numerical explorations

In this section we numerically compute the detection curves and point out the distribution of the limit cycles. The four detection functions can be computed numerically, and for a given h, they depend on u and v, (see tables 1-4). On the other hand, for two given values of u and v, the detection curves can be plotted on the (h, λ)-plane, as illustrated in Fig.4, 5. By the Proposition 1.1 and the detection function graphs, the existence, number and distribution of limit cycles can then be illustrated. We consider here the case $n = 12$.

From (11), we get

$$r_{1,2} = r_{\pm}^2(\theta, h) = \frac{1 \pm \sqrt{1 - hp(\theta)}}{p(\theta)} \tag{13}$$

and from $\dot{\theta} = -1 + r^2 p(\theta) = 0$, we have:

$$\theta_1(h) = \tfrac{1}{2} \arccos\left[\left(b - a + 2\sqrt{a^2 b^2 - ab + (a + b + 2ab)\, h^{-1}}\right) / (a + b + 2ab)\right],$$

$$\theta_2(h) = \tfrac{1}{2} \arccos\left[\left(b - a - 2\sqrt{a^2 b^2 - ab + (a + b + 2ab)\, h^{-1}}\right) / (a + b + 2ab)\right].$$

Using the perturbation terms

$$p\left(x, y\right) = x\left(ux^n + vy^n - b\tfrac{\beta+1}{\mu+1} x^\mu y^\beta - ux^2\right), q\left(x, y\right) = y\left(ux^n + vy^n + bx^\mu y^\beta - vy^2\right)$$
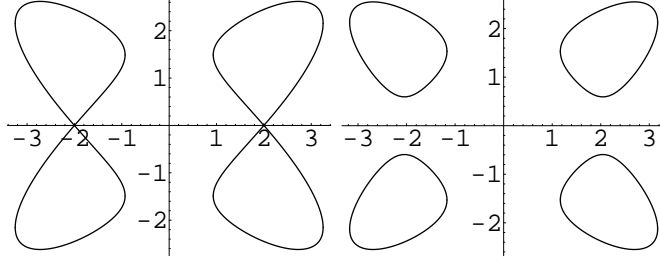
4

Figure 3: a) Four homoclinic orbits connecting the critical points C_1 and C_2 (left) b) Four orbits of type L_4 (right)

we have $\frac{\partial^2 p(x,y)}{\partial x \partial \varepsilon} + \frac{\partial^2 q(x,y)}{\partial y \partial \varepsilon} = (2+n)\left(ux^n + vy^n\right) - 3(ux^2 + vy^2) - 2\lambda$.

Hence, the four detection functions, corresponding to the four closed curves Γ_j^h, $j = 1 - 4$, for the above perturbations are as follows:

$$\lambda_j(h) = \frac{\underset{\Gamma_j^h(D)}{\int} \left[(n+2)\left(ux^n + vy^n\right) - 3(ux^2 + vy^2)\right] dxdy}{2 \underset{\Gamma_j^h(D)}{\int} dxdy}, j = 1 - 4 \qquad (14)$$

For $a = 1/3, b = 1/2$, and $n = 12$, we get by (14) the next four detection functions, in polar coordinates:

$$\lambda_1(h) = \frac{\int_0^{2\pi} \left(r_1^7(\theta, h) g(\theta) - \frac{3}{4} r_1^2(\theta, h) g_1(\theta)\right) d\theta}{\int_0^{2\pi} r_1(\theta, h) d\theta}, \quad -\infty < h < 2, \qquad (15)$$

$$\lambda_2(h) = \frac{\int_0^{2\pi} \left(r_2^7(\theta, h) g(\theta) - \frac{3}{4} r_2^2(\theta, h) g_1(\theta)\right) d\theta}{\int_0^{2\pi} r_2(\theta, h) d\theta}, \quad 0 < h < 2, \qquad (16)$$

$$\lambda_3(h) = \frac{\int_{-\theta_2(h)}^{\theta_2(h)} \left[\left(r_1^7(\theta, h) - r_2^7(\theta, h)\right) g(\theta) - \frac{3}{4}\left(r_1^2(\theta, h) - r_2^2(\theta, h)\right) g_1(\theta)\right] d\theta}{\int_{-\theta_2(h)}^{\theta_2(h)} \left(r_1(\theta, h) - r_2(\theta, h)\right) d\theta}, \quad 2 < h < 3, \qquad (17)$$

5

$$\lambda_4(h) = \frac{\int\limits_{\theta_1(h)}^{\theta_2(h)} \left[\left(r_1^7(\theta,h) - r_2^7(\theta,h)\right) g(\theta) - \frac{3}{4}\left(r_1^2(\theta,h) - r_2^2(\theta,h)\right) g_1(\theta)\right] d\theta}{\int\limits_{\theta_1(h)}^{\theta_2(h)} \left(r_1(\theta,h) - r_2(\theta,h)\right) d\theta}, \quad 3 < h < 8.2, \qquad (18)$$

where $g(\theta) = u\cos^{12}\theta + v\sin^{12}\theta, g_1(\theta) = u\cos^2\theta + v\sin^2\theta$ and $r_{1,2}(\theta,h) = r_\pm^2(\theta,h)$.

Using the expressions (15)-(18) and a Computer Algebra System we find the values of the detection functions $\lambda_i(h), i = 1-4$, recorded in the following tables (1-4). Denote by $\rho = 10^4 u$ and $\omega = 10^4 v$

Table 1
Values of the detection function $\lambda_1(h)$, for $a = 1/3, b = 1/2, n = 12$.

h	$\lambda_1(h)$	h	$\lambda_1(h)$	h	$\lambda_1(h)$
-2	$4.933\rho+ 1.373\omega$	-1.9	$4.862\rho+ 1.352\omega$	-1.8	$4.792\rho+ 1.332\omega$
-1.7	$4.722\rho+ 1.311\omega$	-1.6	$4.653\rho+ 1.291\omega$	-1.5	$4.584\rho+ 1.271\omega$
-1.4	$4.516\rho+ 1.251\omega$	-1.3	$4.448\rho+ 1.231\omega$	-1.2	$4.381\rho+ 1.212\omega$
-1.1	$4.315\rho+ 1.192\omega$	-1.	$4.249\rho+ 1.173\omega$	-0.9	$4.183\rho+ 1.154\omega$
-0.8	$4.118\rho+ 1.135\omega$	-0.7	$4.054\rho+ 1.116\omega$	-0.6	$3.990\rho+ 1.098\omega$
-0.5	$3.926\rho+ 1.079\omega$	-0.4	$3.863\rho+ 1.061\omega$	-0.3	$3.801\rho+ 1.043\omega$
-0.2	$3.739\rho+ 1.025\omega$	-0.1	$3.678\rho+ 1.008\omega$	0	$3.618\rho+ 0.9906\omega$
0.1	$3.558\rho+ 0.9733\omega$	0.2	$3.498\rho+ 0.9562\omega$	0.3	$3.439\rho+ 0.9392\omega$
0.4	$3.381\rho+ 0.9224\omega$	0.5	$3.323\rho+ 0.9058\omega$	0.6	$3.266\rho+ 0.8895\omega$
0.7	$3.210\rho+ 0.8733\omega$	0.8	$3.154\rho+ 0.8573\omega$	0.9	$3.099\rho+ 0.8415\omega$
1.	$3.044\rho+ 0.8259\omega$	1.1	$2.990\rho+ 0.8105\omega$	1.2	$2.937\rho+ 0.7954\omega$
1.3	$2.885\rho+ 0.7805\omega$	1.4	$2.834\rho+ 0.7658\omega$	1.5	$2.783\rho+ 0.7514\omega$
1.6	$2.734\rho+ 0.7373\omega$	1.7	$2.685\rho+ 0.7235\omega$	1.8	$2.638\rho+ 0.7102\omega$
1.9	$2.593\rho+ 0.6974\omega$	2.	$2.553\rho+ 0.6859\omega$		

Table 2
Values of the detection function $\lambda_2(h)$, for $a = 1/3, b = 1/2, n = 12$.

h	$\lambda_2(h)$	h	$\lambda_2(h)$
0.01	-0.001875 u-0.001876 v	0.11	-0.020732 u-0.02083 v
0.21	-0.039766 u-0.0401393 v	0.31	-0.058969 u-0.059813 v
0.41	-0.078305 u-0.079837 v	0.51	-0.097701 u-0.10015 v
0.61	-0.117021 u-0.120612 v	0.71	-0.136046 u-0.140967 v
0.81	-0.154444 u-0.160774 v	0.91	-0.171734 u-0.179321 v
1.01	-0.187236 u-0.195488 v	1.11	-0.200019 u-0.207541 v
1.21	-0.208827 u-0.212808 v	1.31	-0.211988 u-0.207141 v
1.41	-0.207302 u-0.184002 v	1.51	-0.19189 u-0.132774 v
1.61	-0.162016 u-0.0354102 v	1.71	-0.11285 u+0.141107 v
1.81	-0.038213 u+0.465149 v	1.91	0.069632 u+1.1178 v

Table 3
Values of the detection function $\lambda_3(h)$, for $a = 1/3, b = 1/2, n = 12$.

h	$\lambda_3(h)$	h	$\lambda_3(h)$	h	$\lambda_3(h)$
2	$3.0408\rho + 0.8167\omega$	2.02	$3.0446\rho + 0.8175\omega$	2.04	$3.0459\rho + 0.8177\omega$
2.06	$3.0463\rho + 0.8177\omega$	2.08	$3.0462\rho + 0.8175\omega$	2.1	$3.0457\rho + 0.8172\omega$
2.12	$3.0449\rho + 0.8168\omega$	2.14	$3.0438\rho + 0.8164\omega$	2.16	$3.0425\rho + 0.8159\omega$
2.18	$3.0411\rho + 0.8154\omega$	2.2	$3.0396\rho + 0.8148\omega$	2.22	$3.0379\rho + 0.8142\omega$
2.24	$3.0361\rho + 0.8136\omega$	2.26	$3.0342\rho + 0.8130\omega$	2.28	$3.0323\rho + 0.8123\omega$
2.3	$3.0303\rho + 0.8116\omega$	2.32	$3.0283\rho + 0.8110\omega$	2.34	$3.0262\rho + 0.8103\omega$
2.36	$3.0240\rho + 0.8096\omega$	2.38	$3.0219\rho + 0.8089\omega$	2.4	$3.0197\rho + 0.8082\omega$
2.42	$3.0176\rho + 0.8075\omega$	2.44	$3.0154\rho + 0.8068\omega$	2.46	$3.0132\rho + 0.8061\omega$
2.48	$3.0110\rho + 0.8054\omega$	2.5	$3.0089\rho + 0.8047\omega$	2.52	$3.0068\rho + 0.8040\omega$
2.54	$3.0047\rho + 0.8033\omega$	2.56	$3.0026\rho + 0.8027\omega$	2.58	$3.0006\rho + 0.8020\omega$
2.6	$2.9986\rho + 0.8014\omega$	2.62	$2.9967\rho + 0.8008\omega$	2.64	$2.9949\rho + 0.8002\omega$
2.66	$2.9931\rho + 0.7996\omega$	2.68	$2.9915\rho + 0.7991\omega$	2.7	$2.9899\rho + 0.7986\omega$
2.72	$2.9884\rho + 0.7981\omega$	2.74	$2.9871\rho + 0.7976\omega$	2.76	$2.9859\rho + 0.7972\omega$
2.78	$2.9848\rho + 0.7968\omega$	2.8	$2.9839\rho + 0.7965\omega$	2.82	$2.9833\rho + 0.7963\omega$
2.84	$2.9828\rho + 0.7961\omega$	2.86	$2.9826\rho + 0.7959\omega$	2.88	$2.9827\rho + 0.7959\omega$
2.9	$2.9831\rho + 0.7959\omega$	2.92	$2.9840\rho + 0.7961\omega$	2.94	$2.9854\rho + 0.7964\omega$
2.96	$2.9876\rho + 0.7970\omega$	2.98	$2.9909\rho + 0.7978\omega$	3.	$2.9973\rho + 0.7995\omega$

Table 4
Values of the detection function $\lambda_4(h)$, for $a = 1/3, b = 1/2, n = 12$.

h	$\lambda_4(h)$	h	$\lambda_4(h)$	h	$\lambda_4(h)$
3	$2.9973\rho+0.7995\omega$	3.04	$3.0074\rho+0.8022\omega$	3.08	$3.0118\rho+0.8032\omega$
3.12	$3.0140\rho+0.8037\omega$	3.16	$3.0149\rho+0.8037\omega$	3.2	$3.0147\rho+0.8035\omega$
3.24	$3.0138\rho+0.8030\omega$	3.28	$3.0121\rho+0.8024\omega$	3.32	$3.0098\rho+0.8016\omega$
3.36	$3.0070\rho+0.8006\omega$	3.4	$3.0038\rho+0.7995\omega$	3.44	$3.0001\rho+0.7982\omega$
3.48	$2.9960\rho+0.7969\omega$	3.52	$2.9915\rho+0.7954\omega$	3.56	$2.9867\rho+0.7939\omega$
3.6	$2.9816\rho+0.7922\omega$	3.64	$2.9762\rho+0.7905\omega$	3.68	$2.9706\rho+0.7887\omega$
3.72	$2.9646\rho+0.7868\omega$	3.76	$2.9584\rho+0.7849\omega$	3.8	$2.9520\rho+0.7829\omega$
3.84	$2.9453\rho+0.7808\omega$	3.88	$2.9384\rho+0.7787\omega$	3.92	$2.9313\rho+0.7765\omega$
3.96	$2.9240\rho+0.7742\omega$	4.	$2.9165\rho+0.7719\omega$	4.2	$2.8764\rho+0.7596\omega$
4.4	$2.8322\rho+0.7461\omega$	4.6	$2.7847\rho+0.7317\omega$	4.8	$2.7341\rho+0.7165\omega$
5.	$2.6808\rho+0.7005\omega$	5.2	$2.6250\rho+0.6838\omega$	5.4	$2.5671\rho+0.6665\omega$
5.6	$2.5072\rho+0.6487\omega$	5.8	$2.4455\rho+0.6304\omega$	6.	$2.3820\rho+0.6116\omega$
6.2	$2.3171\rho+0.5924\omega$	6.4	$2.2507\rho+0.5729\omega$	6.6	$2.1830\rho+0.5530\omega$
6.8	$2.1141\rho+0.5327\omega$	7.	$2.0440\rho+0.5122\omega$	7.2	$1.9729\rho+0.4914\omega$
7.4	$1.9008\rho+0.4704\omega$	7.6	$1.8278\rho+0.4491\omega$	7.8	$1.7540\rho+0.4277\omega$
8.	$1.6794\rho+0.4060\omega$	8.2	$1.6041\rho+0.3842\omega$		

From the tables (1-4) we have the four detection functions, three of which are shown in Fig.4, 5. The values of λ_2 are not plotted because they are too small in comparison with the other values. From Proposition 1.1, and Fig.4, 5, one gets:
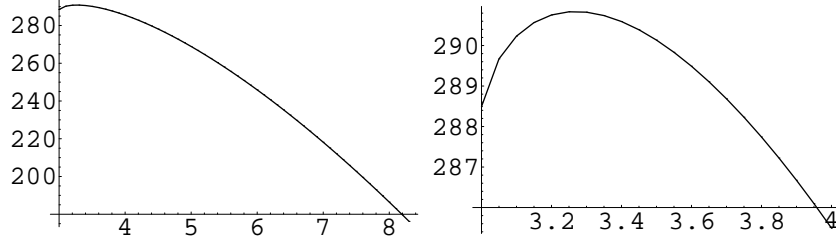
Figure 4: Detection curve λ_4 of the system , for $\quad a = \frac{1}{3}, b = \frac{1}{2}, n = 12, u = 0.007$ and $v = -0.028$.
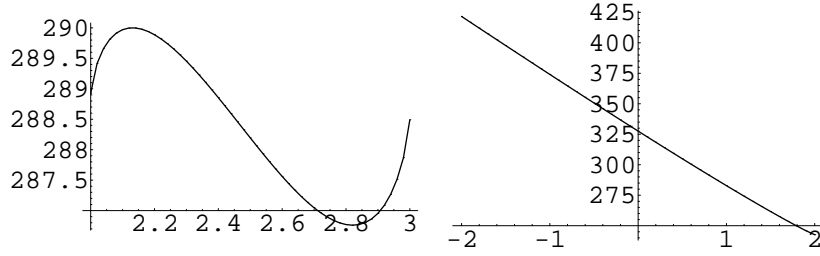

Figure 5: Detection curves λ_3 (left), λ_1 (right) of the system (1), for $\quad a = \frac{1}{3}, b = \frac{1}{2}, n = 12, u = 0.007$ and $v = -0.028$

THEOREM 3.1 *For* $a = \frac{1}{3}, b = \frac{1}{2}, n = 12, u = 0.007$ *and* $v = -0.028$ *and* $0 < \varepsilon \ll 1$, *we have the following distribution of the limit cycles:*

a) If $176.22 < \lambda < 242.6$, *the system (1) has at least four limit cycles, one in the neighborhood of each orbit of type* Γ_4^h, *Fig.6a),*

b) If $242.6 < \lambda < 286.76$, *the system (1) has at least five limit cycles, one in the neighborhood of each orbit of type* Γ_4^h *and* Γ_1^h, *Fig.6b),*

c) If $286.76 < \lambda < 288.49$, *the system (1) has at least nine limit cycles, two in the neighborhood of each orbit of type* Γ_3^h, *and one in the neighborhood of each orbit of type* Γ_4^h, Γ_1^h, *Fig.6c),*

d) If $288.49 < \lambda < 288.92$, *the system (1) has at least eleven limit cycles, two in the neighborhood of each orbit of type* Γ_4^h *and one in the neighborhood of each orbit of type* Γ_3^h, Γ_1^h, *Fig.7a),*

e) If $288.92 < \lambda < 289.99$, *the system (1) has at least thirteen limit cycles, two in the neighborhood of each orbit of type* Γ_4^h, Γ_3^h *and one in the neighborhood of the orbit of type* Γ_1^h, *Fig.7b),*

f) If $289.99 < \lambda < 290.82$, *the system (1) has at least nine limit cycles, two in the neighborhood of each orbit of type* Γ_4^h *and one in the neighborhood of the orbit of type* Γ_1^h, *Fig.7c) .*

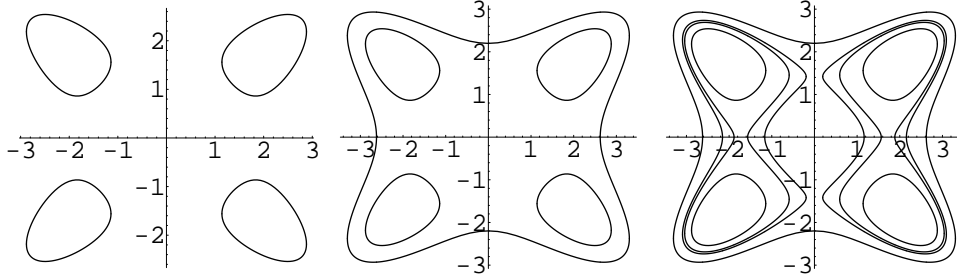From Fig.4, 5 we could obtain more results but we listed only the important cases.

Figure 6: Distribution diagram corresponding to: a) four (left), b) five (middle), c) nine (right) limit cycles of the system (1)
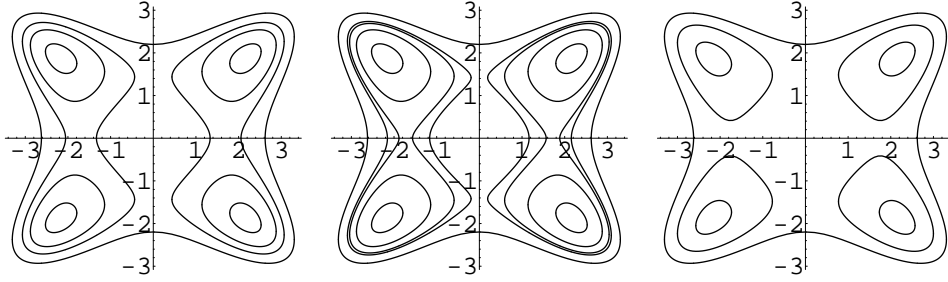

Figure 7: Distribution diagram corresponding to: a) eleven (left), b) thirteen (middle), c) nine (right) limit cycles of the system (1)

4 Conclusion

The system (1) corresponding to $a = \frac{1}{3}, b = \frac{1}{2}, n = 12, u = 0.007, v = -0.028, 0 < \varepsilon \ll 1$, and $288.49 < \lambda < 288.92$, has at least eleven limit cycles while for $288.92 < \lambda < 289.99$ it has at least thirteen limit cycles. The Abelian integral method was used. Through numerical explorations we have drawn the shape of the graphs of the detection functions, from which we determined the number and distribution of limit cycles. A natural question is: Is it possible to obtain more limit cycles for higher perturbations?

5 Acknowledgements

References

[1] Li JB., Liu ZR., Bifurcation set and limit cycles forming compound eyes in a perturbed Hamiltonian system, Publ.Math. (1991), 35, 487-506.

[2] Cao H., Liu Z., Jing Z., Bifurcation set and distribution of limit cycles for a class of cubic Hamiltonian system with higher-order perturbed terms, Chaos, Solitons and Fractals (2000), 11, 2293-2304.

[3] Tang M., Hong X., Fourteen limit cycles in a cubic Hamiltonian system with nine-order perturbed term, Chaos, Solitons and Fractals (2002), 14, 1361-1369.

[4] Chows SN., Li C., Wang D., Normal Forms and Bifurcation of Planar Vector Fields, Cambridge University Press, Cambridge, 1994.

[5] Yanqian Y., Theory of Limit Cycles, Translations of Math. Monographs, vol. 66, Amer. Math. Soc.,Providence, RI, 1986.

[6] Li CF., Li JB., Distribution of limit cycles for planar cubic Hamiltonian systems, Acta Math Sinica, (1985), 28, 509-521.

[7] Li J., Huang Q., Bifurcation of limit cycles forming compound eyes in the cubic system, Chinese Ann. Math., (1987), 8B(4), 391-403.

[8] Gh. Tigan, Eleven limit cycles in a Hamiltonian system, The 5-th Conference of Balkan Society of Geometers, Mangalia, 2005.

[9] Gh. Tigan, Thirteen limit cycles for a class of Hamiltonian systems under seven-order perturbed terms, Chaos, Solitons and Fractals, Elsevier Ref. CHAOS 4182, in press.

[10] Gh. Tigan, Existence and distribution of limit cycles in a Hamiltonian system, Applied Mathematics E–Notes, Taiwan, to appear.

[11] Gh. Tigan, Analysis of a perturbed Hamiltonian system, in review.

[12] Viano M., Llibre J., Giacomini H., Arbitrary order bifurcations for perturbed Hamiltonian planar systems via the reciprocal of an integrating factor, Nonlinear Analysis, (2002), 48, 117-136.

[13] Li JB.,Liu ZR., On the connection between two parts of Hilbert's 16-th problem and equvariant bifurcation problem, Ann. Diff. Eqs., (1998), 14(2), 224-35.

[14] Giacomini H., Llibre J., Viano M., On the nonexistence, existence and uniqueness of limit cycles, Nonlinearity, (1996), 9, 501-516.

[15] Andronov A.A., Theory of bifurcations of dynamical systems on a plane, Israel program for scientific translations, Jerusalem 1971.

[16] Blows T.R., Perko L.M., Bifurcation of limit cycles from centers and separatrix cycles of planar analytic systems, SIAM Rev., (1994), 36, 341-376.

[17] Giacomini H., Llibre J., Viano M., On the shape of limit cycles that bifurcate from Hamiltonian centers, Nonlinear Anal. Theory Methods Appl., (1997), 41, 523-537.